Hydrodynamic modelling of hydrostatic magnesium extrusion

E. Moodij, M.B. de Rooij and D.J. Schipper
Lab. for Surface Technology and Tribology
Faculty of Engineering Technology
University of Twente
P.O. Box 217, 7500AE Enschede
The Netherlands
E-mail: e.moodij@utwente.nl

Abstract

Wilson's hydrodynamic model of the hydrostatic extrusion process is extended to meet the geometry found on residual billets. The transition from inlet to work zone of the process is not considered sharp as in the model of Wilson but as a rounded edge, modelled by a parabolic function. It is shown that this rounded edge has a considerable influence on the predicted film thickness. Furthermore, it is shown that for hydrostatic extrusion of magnesium with castor oil as pressure medium, it is not possible to generate full film lubrication in the work zone of the hydrostatic extrusion process.

1. INTRODUCTION

Hydrostatic extrusion is a process where the billet is surrounded by a fluid medium. The deforming pressure is not directly applied onto the billet but on the fluid. This results in a hydrostatic pressure instead of only a one-sided pressure as in conventional extrusion. The main advantages are the reduced friction level at the billet-container interface and the increased deformability of materials.

Magnesium is a material which nowadays has a considerable interest. It is used because of its low specific mass, which is 2/3 of aluminium and 1/5 of steel. It is however more expensive than aluminium. One of the problems with magnesium is that it is difficult to deform due to its HCP crystal structure. Due to the hydrostatic pressure and the deformation characteristics, hydrostatic extrusion is a suitable process to deform magnesium.

The tribological system for hydrostatic extrusion has mainly been studied in the seventies. Wilson & Walowit (1971) developed a hydro-dynamic lubrication theory for continuous axi-symmetrical deformation processes based on the Reynolds equation. Hillier (1966) and Kauljalgi (1970) modelled the film thickness based on the minimum work technique, which does not account for the hydrodynamic effects in the inlet zone.

As will be shown later, the model of Wilson & Walowit (1971) gives an extremely low value for the film thickness in hydrostatic extrusion. This may be explained by the abrupt transition from inlet to work zone in this model. From residual billets it is observed that this transition is formed by a round edge, which may have a positive effect on the film thickness. In this paper, the model of Wilson & Walowit is extended to meet this geometry and different calculations are performed to investigate the influence of several process parameters. Furthermore, the calculations are used to investigate in which lubrication regime the process is operating.

As an indicator for the relevant lubrication regime in which the process is operating, the quantity h/σ_{und}, the film thickness over the undeformed roughness (RMS), is used. If $h/\sigma_{und} > 3$ the system is considered to operate in the full film lubrication regime, if $h/\sigma_{und} < 0.1$ boundary lubrication is expected. In the intermediate regime $0.1 < h/\sigma_{und} < 3$ the mixed lubrication regime is more likely.

2. MODELLING

The hydrostatic extrusion process is divided into three zones, an inlet zone, a work zone and an outlet zone as shown in Figure 1. Wilson & Walowit (1971) modelled the film thickness in the inlet zone with the Reynolds equation based on only the wedge term,

$$\frac{\partial}{\partial x}\left(\frac{h^3}{\eta}\frac{\partial p}{\partial x}\right) = -6(U_1 + U_2)\frac{\partial h}{\partial x} \qquad (1)$$

with p the pressure, h the film thickness, η the viscosity of fluid and U_1 and U_2 the velocities of surfaces 1 and 2 respectively, in this case the billet and the die. The boundary conditions are $p = q$ for $x \to \infty$ and $p = q + \bar{\sigma}$ at $x = x_0$, the transition point from the inlet to the work zone. There the billet starts to deform plastically and therefore the pressure has to be equal to the hydrostatic pressure plus the flow stress of the billet material. The viscosity is modelled with the Barus equation, see Appendix A, which leads to

$$h_0 = \frac{3U_1 \alpha \eta_0 e^{\alpha q}}{\left(1 - e^{-\alpha \cdot \bar{\sigma}}\right) \tan\theta}, \qquad (2)$$

with h_0 the (central) film thickness at the transition point from inlet to work zone, θ the angle between the die and the billet and α the Barus pressure coefficient.

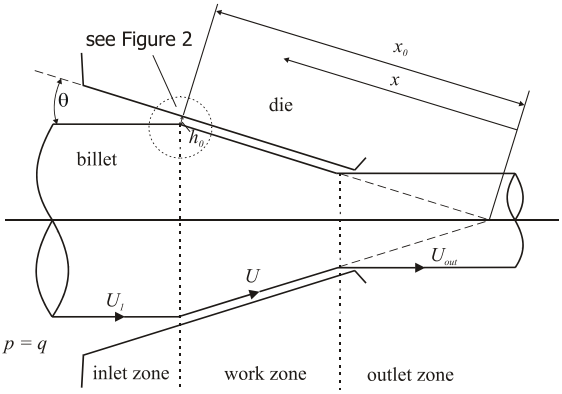

Figure 1 The generalized extrusion process, based upon Wilson & Walowit (1971).

Wilson & Walowit (1971) showed furthermore that the film thickness is decreasing in the work zone, $h = h_0 \cdot x / x_0$. So, h_0 is a good measure for the lubrication regime in the hydrostatic extrusion process. This theory applied to hydrostatic extrusion of magnesium leads to a central film thickness h_0 of the order 10^{-10} to 10^{-9} m. For the process parameters given in Table 1, h_0 is $3.4 \cdot 10^{-10}$ m. This film thickness clearly indicates boundary lubrication regime, $h/\sigma_{und} << 0.1$.

2.1. Adapted model

Residual billets from the hydrostatic extrusion process show that the transition from inlet to work zone is not abrupt, but is formed by a rounded edge. This rounded edge can contribute to an increase in film thickness, because the effective wedge in the inlet zone changes and therefore also the film thickness. The round edge is modelled with a parabolic function

$$h(x) = \frac{(x - x_0)^2}{2R} + h_0 \quad \text{for } x > x_0 \qquad (3)$$

with x and x_0 defined as in Figure 1 and R the radius of the rounded edge. The boundary conditions result from the pressure constraints and are the same as used in Wilson's model. With the Barus viscosity equation and the geometry of (3), equation (1) can be solved analytically; the result can be found in Appendix B. However the acting pressure is very high and therefore the use of the Barus equation is questionable. Numerical calculations are performed with the Roelands viscosity equation, see Appendix A.

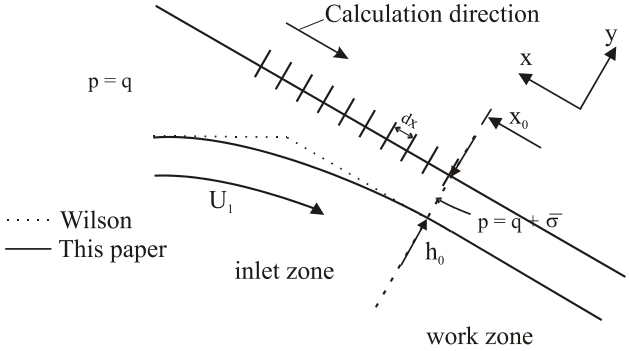

Figure 2 Segments finite difference method.

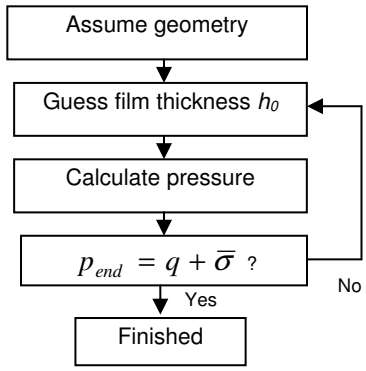

Figure 3 Iteration loop of the finite difference method.

A finite difference numerical program is made using Matlab to be able to calculate the film thickness for this situation. The program is an iteration loop on the central film thickness h_0. First the geometry is assumed, e.g. the parabolic model as in eq. (3) and the film thickness, h_0, is guessed. The calculating area is divided into a beforehand specified number of segments. Consecutively, the pressure is calculated in the film in each of these segments, starting from the hydrostatic pressure, $x = \infty$, to the transition point from inlet to work zone at $x = x_0$, see also Figure 2. The pressure, $x = x_0$, is already known and equal to $q + \bar{\sigma}$, so

the calculated value is compared to the known value. If the calculated value is higher than $q + \overline{\sigma}$ the estimation of h_0 is increased and vice versa until the calculated value is close enough to the known value. The iteration loop is illustrated in Figure 3.

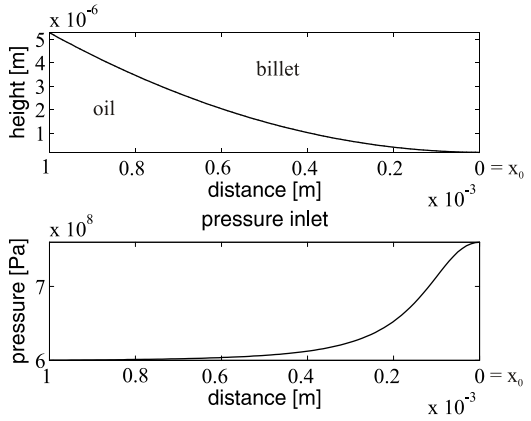

Figure 4 Example output of the numerical program.

The program calculates the film thickness, the pressure and also the viscosity, assuming that the die does not deform. Figure 4 shows an example of an output of the finite difference program. In the upper graph the shape of the film can be seen and therefore also the shape of the billet. The bottom graph shows the pressure increase in the lubricant. From both graphs it can be seen that the pressure increase only takes place in the last part of the inlet zone. For this case, the calculation domain is set to the last 1 mm of the inlet zone, which is clearly enough for this calculation. For some calculations it is necessary to increase the calculation domain.

Table 1 Data set for magnesium extrusion using castor oil.

Symbol	Value	Description
q	6000 bar	extrusion pressure
r_1	73 mm	billet diameter
r_2	8 mm	end diameter
U_1	8.8 mm/s	velocity of the billet
θ	45˚	semi die angle
R	0.1 m	round-off radius of the billet
$\overline{\sigma}$	160 MPa	flow stress magnesium (AZ31)
T	200˚C	oil temperature
η_0	18.6 mPa·s	viscosity lubricant at 1 bar at 100 ˚C
α^1	$7 \cdot 10^{-9}$ Pa^{-1}	viscosity pressure coefficient
z	0.43	Roelands pressure-viscosity coefficient
σ_{und}	6 µm	RMS of a Mg billet

[1] This Barus viscosity coefficient is fitted onto the Roelands equation in the appropriate pressure regime.

3. RESULTS

Calculations are performed for a reference set of variables, see Table 1. Unless stated otherwise, all calculations are conducted with the Roelands viscosity relation. The central film thickness of this reference data set is $1.6 \cdot 10^{-8}$ m. For each set of calculations, one of the parameters is changed to investigate the influence of that particular parameter.

3.1. Velocity of the billet

The first parameter investigated is the velocity of the billet. It is varied from 1.8 mm/s to 31.3 mm/s, these are all values actually used on a hydrostatic extrusion press. The resulting film thicknesses can be found in Figure 5. From this figure it can be seen that increasing the velocity of the billet results in an increase in film thickness. The effect is however not as significant as in Wilson's model, there $h_0 \sim U_1$ and here $h_0 \sim U_1^{2/3}$.

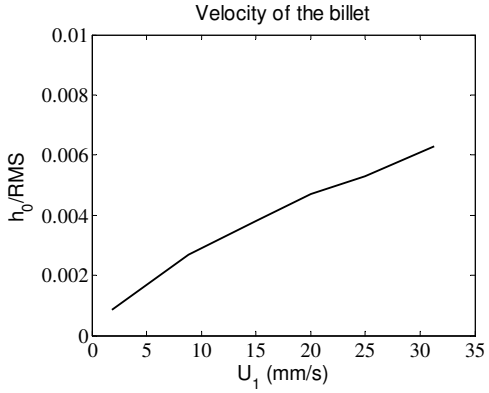

Figure 5 Influence of the velocity of the billet.

3.2. Hydrostatic pressure

The next parameter investigated is the hydrostatic extrusion pressure in the press. The hydrostatic pressure for magnesium extrusion is typically between 0.5 GPa and 1.2 GPa, results can be found in Figure 6. In this figure it can be seen that increasing the hydrostatic pressure has a positive effect on the film thickness.

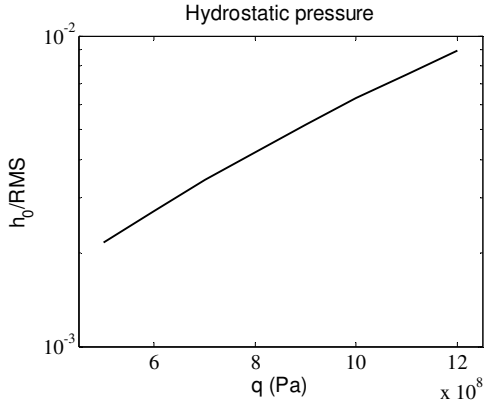

Figure 6 Influence of hydrostatic extrusion pressure.

3.3. Temperature of the oil

The last process parameter investigated is the temperature of the oil. The oil is brought in the press at room temperature, the billet however is heated up to about 200 ˚C before being put in the press and the die is even warmer, about 350 ˚C. The result is a fast changing temperature of the oil in the initial stage of the process. Due to the influence of the temperature on the viscosity of the oil it is however an important process parameter. The results can be found in Figure 7. These results only incorporate the influence of temperature on the viscosity of the castor oil. Other effects like the influence of temperature on the flow stress of the magnesium are neglected in this work. Figure 7 shows that within the temperature range studied, hydrodynamic effects can be neglected.

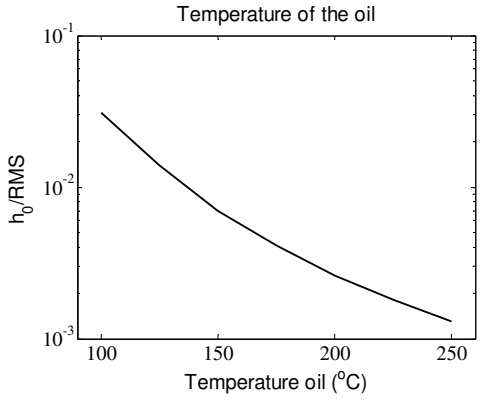

Figure 7 Influence of the temperature of the oil.

Calculations are also performed for different base viscosities, $\eta_{0,}$ the viscosity at atmospheric pressure. The results can be found in Figure 8, which has double logarithmic scale. These two effects are in fact the same; if the temperature of the oil is increasing, the base viscosity η_0 will decrease. So, apart from the orientation and the scale Figures 7 and 8 are comparable, $h_0 \sim \eta_0^{2/3}$.

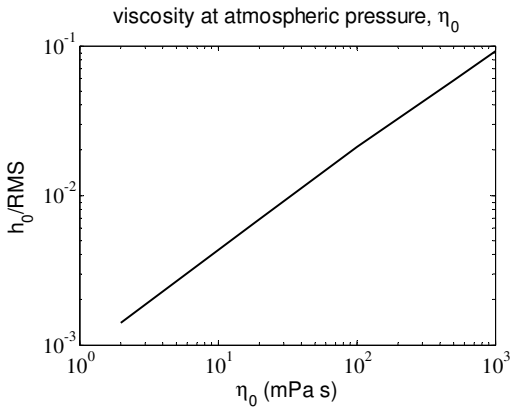

Figure 8 Influence of the viscosity at atmospheric pressure, double logarithmic scale.

3.4. Billet geometry

Furthermore, the influence of the geometry of the billet is investigated. The round-off radius of the billet at the transition from inlet zone to work zone is not exactly known. Therefore the calculations are done for a wide range of values. The results of the calculations are plotted in Figure 9, i.e. $h_0 \sim R^{1/3}$.

Film thickness calculations were also done with different die angles, θ, however no change of h_0 was found. This is logical because the pressure increase only takes place in the last few millimetres of the inlet zone and this area is always determined by the round-off radius and not by the actual die angle θ.

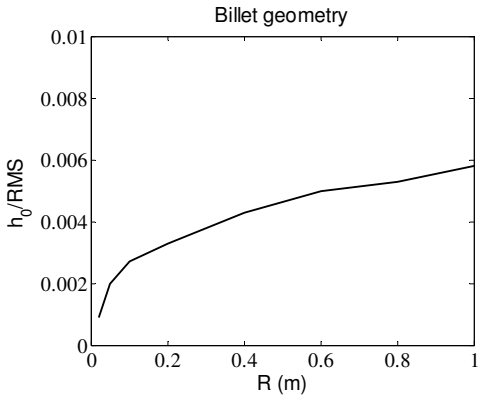

Figure 9 Influence of the round-off radius of the billet.

3.5. Lubricant

As shown in Section 3.3 the viscosity of the oil is a very important parameter in these calculations. Therefore calculations were conducted to investigate the importance of the used value of the parameters for the different viscosity models,

Roelands and Barus. At first the pressure-viscosity coefficient, z, of the Roelands equation was varied in Figure 10. According to Booser (1997) the z value for castor oil is 0.43. These calculations were performed with a temperature of 150˚C.

From Figure 10 it can be seen that z is indeed an important parameter in this model. With an increasing value of z from 0.43 to 0.9 the film thickness increases from the order of 10^{-8} to 10^{-6} m (micrometer scale), which is similar to the scale of the roughness. The before mentioned z value for castor oil is extremely low, usually z varies between 0.6 and 1.0, which would increase the film thickness into the order of the roughness.

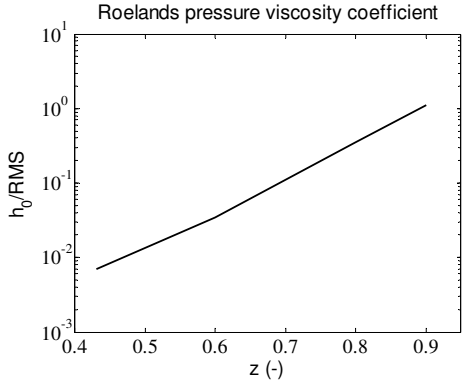

Figure 10 Influence of the pressure-viscosity coefficient *z* in Roelands' viscosity model, logarithmic scale.

The pressure coefficient α for the Barus equation was only found for 40 ˚C which is $1.78 \cdot 10^{-8}$ Pa^{-1}, (Schipper & Ten Napel, 1998). For higher temperatures this value is decreasing. If the Barus equation is fitted onto the Roelands equation for 0.6 GPa and 150 ˚C the pressure coefficient is $4 \cdot 10^{-9}$ Pa^{-1}.

Calculations are performed with the analytical model given in Appendix B for different 'standard' α values at 150 ˚C. The same calculations are performed with the model of Wilson; both results are shown in Figure 11.

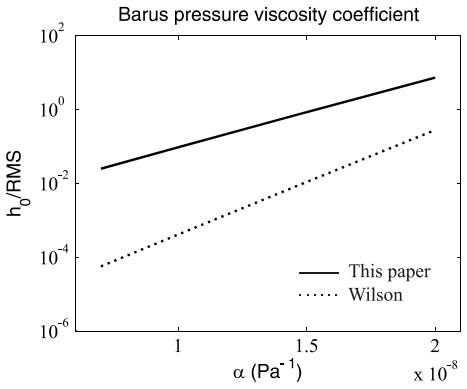

Figure 11 Influence of the pressure-viscosity coefficient α of Barus.

4. DISCUSSION AND CONCLUSION

The original Wilson model predicts values of the central film thickness in hydrostatic extrusion of magnesium in the order of 10^{-10} m. This model has been adapted by fitting the geometry of a real billet. Residual billets were inspected and a round edge on the transition from the inlet to the work zone was found. This round-off radius was incorporated in the model by a parabolic function. For the Barus viscosity equation the resulting model is solved analytically. Also, a numerical finite difference program is made, using Matlab, to be able to calculate film thicknesses for both the Barus and the Roelands viscosity equation with this geometry.

If the same dataset is used with this round-off radius instead of the sharp edge of Wilson, the predicted film thickness increases from 10^{-10} m to 10^{-8} m. To further investigate the difference between the two models, the pressure-viscosity coefficient α is varied. From Figure 11 it can be seen that for increasing α, the difference between the two models decreases. This can be explained as follows: The film thickness is governed by the wedge in the geometry but also by the increase of the viscosity due to the pressure rise. If α increases, the lubricant reacts more to the pressure increase and therefore the relative importance of the shape of the wedge will decrease. So, for high α the Wilson's model with the sharp edge converges to the model presented in this paper.

Furthermore, the influence of the process parameters is investigated. The process parameters do influence the expected film thickness but always within the boundary lubrication regime, $h_0/\sigma_{und} << 0.01$. Only by decreasing the temperature it is possible to generate an h_0/σ_{und}-ratio larger than 0.1. In deformation processes of magnesium this temperature regime is not preferred because above 200 °C pyramid sliding planes become thermally activated and magnesium is easier to deform (Doege & Dröder, 2001).

If the viscosity coefficients are varied, a film thickness of several times the roughness is predicted and full film lubrication can occur. The calculations for z and α show that the film thickness is of the order of the roughness, and even a few times the roughness can be achieved with higher pressure coefficients. The effect of the base viscosity is also obvious, but not as extreme as the pressure coefficient. This indicates that the temperature effect is less pronounced than the

pressure effect. One has to keep in mind that the viscosity models are used at their limits. The pressure may be too high for these models. This implies that it is very important to know the exact behaviour of castor at the pressures and temperatures acting in this situation. It is questionable if the value of $z = 0.43$ from Booser (1997) is applicable for these pressures. The system might benefit from using a different oil with a higher pressure-viscosity coefficient.

Furthermore, it has to be mentioned that the roughness of the billet is decreasing during the extrusion process, while all results mentioned are calculated with the undeformed roughness. If the roughness is decreasing, h_0/σ is increasing so there might be actually mixed lubrication even if h_0/σ_{und} indicates boundary lubrication.

5. ACKNOWLEDGMENTS

The authors gratefully acknowledge Hydrex Materials BV for the material supplied and their support. The Innovation Directed Research Programme on Surface Technology is gratefully acknowledged for their financial support.

6. REFERENCES

Booser, E.R. ed. (1997), *Tribology data handbook, STLE, CRC Press*, New York, USA.

Doege, E. and Dröder, K. (2001), *Sheet metal forming of magnesium wrought alloys – formability and process technology*, J. of Mat. Proc. Techn., 115, 14-19.

Hillier, M.J. (1966), *A hydrodynamic model of hydrostatic extrusion*, Int. J. of Prod. Research, 5 (2), 171-181.

Kaujalgi, V.B. (1970), *An hydrodynamic model of hydrostatic extrusion with variable lubricant film thickness*, Int. J. of Prod. Research, 8 (4), 315-323

Schipper, D.J. and Ten Napel, W.E. (1998), *The effects of the viscosity-pressure behaviour of lubricant on the film thickness in elasto-hydrodynamically lubricated contacts*, Tribology for energy conservation, Dowson D. (Ed.), *Proc. of the 24th Leeds-Lyon Symposium*, London, 4th-6th Sept, 1997, 455-464.

Wilson, W.R.D. and Walowit, J.A. (1971), *An isothermal hydrodynamic lubrication theory for hydrostatic extrusion and drawing processes with conical dies*, J. of Lubrication Techn., 92, 69-74.

Appendix A

The Barus viscosity equation

$$\eta = \eta_0 e^{\alpha p} \tag{A-1}$$

with η the dynamic viscosity, η_0 the dynamic viscosity at ambient pressure, α the viscosity-pressure coefficient and p the pressure.

The Roelands viscosity equation

$$\eta = \eta_0 \exp\left[\left\{\left(1+\frac{p}{p_r}\right)^z - 1\right\}\ln\left(\frac{\eta_0}{\eta_\infty}\right)\right] \tag{A-2}$$

with p_r a reference pressure of $1.96 \cdot 10^8$ Pa, z the pressure-viscosity coefficient and η_∞ a constant, $6.315 \cdot 10^{-5}$ Pa·s.

The relation between α and η_0 and z reads

$$\alpha = \ln\left(\frac{\eta_0}{\eta_\infty}\right)\cdot\frac{z}{p_r}. \tag{A-3}$$

Appendix B

The Reynolds equation, (1), with the parabolic billet geometry, (3), and Barus viscosity equation, (A-1), is solved analytically. The pressure reads

$$p(x') = -\frac{1}{\alpha}\ln\left\{6\alpha\eta_0 U_1 G(x') + e^{-\alpha\cdot q} - \frac{3}{8}\sqrt{2}\pi\alpha\eta_0 U_1 \frac{\sqrt{R}}{h_0\sqrt{h_0}}\right\}$$

with $x' = x - x_0$ and

$$G(x') = -\frac{R^2 x'}{\left(2h_0 R + (x')^2\right)^2} + \frac{R\cdot x'}{4h_0\left(2h_0 R + (x')^2\right)} + \frac{\sqrt{2}R\arctan\left(\frac{x'\sqrt{2}}{2\sqrt{h_0 R}}\right)}{8h_0\sqrt{h_0 R}}.$$

This results in a film thickness of

$$h_0 = \left(\frac{3\sqrt{2}\pi\alpha\eta_0 U_1\sqrt{R}e^{\alpha\cdot q}}{8\left(1-e^{-\alpha\cdot\sigma}\right)}\right)^{2/3} \tag{B-1}$$